Available online at www.sciencedirect.com
SCIENCE DIRECT
Journal of Colloid and Interface Science 278 (2004) 115–125
JOURNAL OF Colloid and Interface Science
www.elsevier.com/locate/jcis

Heteroaggregation, repeptization and stability in mixtures of oppositely charged colloids

M. Raşa [a,*], A.P. Philipse [a], J.D. Meeldijk [b,c]

[a] *Van 't Hoff Laboratory for Physical and Colloid Chemistry, Debye Institute, Utrecht University, Padualaan 8, 3584 CH Utrecht, The Netherlands*
[b] *Department of Cell Biology, Utrecht University, Padualaan 8, 3584 CH Utrecht, The Netherlands*
[c] *Debye Institute, Utrecht University, Padualaan 8, 3584 CH Utrecht, The Netherlands*

Received 10 November 2003; accepted 18 May 2004

Available online 15 June 2004

Abstract

We report a study of mixtures of initially oppositely charged particles with similar size. Dispersions of silica spheres (negatively charged) and alumina-coated silica spheres (positively charged) at low ionic strength, mixed at various volume ratios, exhibited a surprising stability up to compositions of 50% negative colloids as well as spontaneous repeptization of particles from the early-stage formed aggregates. The other mixtures were found to contain large heteroaggregates, which were imaged using cryogenic electron microscopy. Electrophoretic mobility, electrical conductivity, static and dynamic light scattering and sedimentation were studied as a function of volume fraction of the mixed dispersions to investigate particle interactions and elucidate the repeptization phenomenon.

Keywords: Heteroaggregation; Heterocoagulation; Repeptization; Colloidal dispersions; Silica; Electrophoresis; Cryogenic electron microscopy

1. Introduction

Aggregation in colloidal dispersions containing two different types of particles may take place between the same type of particles (homoaggregation) or between unlike particles (heteroaggregation). Several studies have been carried out on systems containing oppositely charged particles [1–4]. It was shown [1] that the relative size of the particles determines the morphology of aggregation: if there is a significant difference in size, the small particles are adsorbed onto the large particles but if particles have comparable size, growth of large fractal clusters may take place. Heteroaggregation, which occurs together with or without homoaggregation was studied in [2] where the morphology of clusters was observed after performing electron microscopy on dried samples. However, in the process of drying the cluster morphology may change and clusters may even form due to capillary forces induced by a receding liquid front. Early stage fractal cluster formation was analyzed in detail in [3]. Kinetics of heteroaggregation (mainly in the early stage) also received much attention [5–7]. In [7] heteroaggregation versus homoaggregation was studied by varying the ionic strength. Simulation of growth of large heteroaggregates, determination of fractal size of heteroaggregates and the effect of added electrolyte were recently presented in [4]. Papers [8,9] review the experimental and theoretical studies on heteroaggregation, respectively.

We report in this paper the surprising stability of initially oppositely charged particle mixtures with a (initially) negative dispersion content between 0 and 50%. Commercially available aqueous dispersions of positively and negatively charged silica particles were used. The dispersions were dialyzed against ethanol, so that only the low ionic strength regime is considered. In such a case, homoaggregation is initially inhibited. After the mixtures were studied at low ionic strength, salt effects were investigated. The size of the mixed spherical particles was approximately the same. Similar types of particles as in [3] were used.

The repeptization observed in the stable mixtures, consisting of spontaneous redispersion of particles from heteroaggregates, was investigated by electrophoresis, conductivity measurements, dynamic light scattering and sedimentation experiments. The mixtures containing more than 50%

* Corresponding author. Fax: +31-30-2533870.
E-mail address: m.rasa@chem.uu.nl (M. Raşa).

0021-9797/$ – see front matter
doi:10.1016/j.jcis.2004.05.020

Table 1
Samples obtained by mixing the negative and positive particle dispersions

Sample	S1	Se	Sd	Sc	Sb	Sa	S2	S3	S4	S5
Positive Ludox (ml)	0	0.001	0.01	0.025	0.05	0.1	0.25	0.5	0.75	1
Negative Ludox (ml)	5	5	4.99	4.975	4.95	4.9	4.75	4.5	4.25	4
Φ_d (%)	100	99.9	99.8	99.5	99	98	95	90	85	80
Sample	S6	S7	S8	S9	S10	S11	S12	S13	S14	S15
Positive Ludox (ml)	1.5	2	2.5	3	3.5	4	4.25	4.5	4.75	5
Negative Ludox (ml)	3.5	3	2.5	2	1.5	1	0.75	0.5	0.25	0
Φ_d (%)	70	60	50	40	30	20	15	10	5	0

The mass fraction of both dispersions was 4% (corresponding to 2 vol%). Φ_d is the volume of the negative particle dispersion relative to the total volume of mixtures, which was 5 ml.

negative dispersion are strongly aggregated. Cluster formation was studied by cryogenic transmission electron microscopy (cryo-TEM) because this technique images the clusters in situ and avoids drying effects which may complicate the conventional TEM pictures used so far. Even in the case of aggregated samples, our observations at extreme volume ratio of positive and negative particle dispersions were different from those presented in [3], where the aggregation was terminated at an early stage.

2. Materials and methods

2.1. Sample description

The colloids in our experiments were originally commercial aqueous dispersions (DuPont) of negatively charged silica particles (Ludox HS-40) and positively charged silica particles (Ludox CL). In what follows these dispersions will be referred to as the negative dispersion and positive dispersion, respectively. The positive charge is due to a thin layer of alumina which covers the silica core. According to the suplier's information, the average diameter of particles is 12 nm. The counterions in the negative and positive Ludox dispersions are Na^+ and Cl^-, respectively, while the co-ions are OH^- and H^+, respectively. The study of mixtures of positive and negative particles was carried out with samples prepared as follows.

First series of mixtures (series I). It was previously observed [10] that ethanol addition to negative Ludox particles flocculates the suspension because of the presence of dissolved silica which precipitates in ethanol. Consequently, an ion exchange procedure is required to remove soluble silica. The particles (contained in 200 ml of dispersion diluted to a weight concentration of 20%) were successively mixed with 100 g Dowex 50WX8 sulfonic acid resins and Dowex 1X8 quaternary ammonium resin. The resins were conditioned according to [11] and were stirred with the aqueous dispersion several hours. The resulting dispersion was filtered to remove flocs, diluted with ethanol, and dialyzed against ethanol (technical grade) for one week. An attempt to apply resins to Ludox CL failed: the dispersion gelated when it was mixed with the alkaline resins, probably because the positive Ludox particles are not stable at basic pH. Fortunately, ion exchange turned out to be unnecessary for the positive Ludox particles; they are stable if ethanol is added in any amount, apparently because the alumina coating suppresses the silica solubility. Consequently, the ion concentration in the positive particle dispersion could be reduced only through dialysis. Mixtures of the two type of dispersions containing 4 wt% particles (corresponding to approximately 2 vol%), were made according to Table 1. After injecting one dispersion into the other the mixture was stirred half a minute.

A second series of mixtures (series II) was prepared to check the reproducibility of the observations made on series I, and to obtain dust free samples for experiments in which light scattering is involved. The positive dispersion was subjected to dialysis as previously, but now for a longer period of 16 days. The negative dispersion was subjected to ion exchange using AG 501-X8 (Bio-Rad) mixed bed resins. We used 250 ml of the as-received dispersion, which was subsequently diluted to a weight concentration of 20%, and mixed with approximately 30 g of mixed resins and stirred for one hour. The procedure was repeated once more with fresh resins. Then the dispersion was diluted with ethanol and dialyzed against ethanol for one week. The dispersions based on ethanol were centrifuged three times (2000 rpm, 1 h) to remove aggregates and dust. The mixtures were prepared in a dust free environment and dilutions were made using filtered ethanol. The same composition scheme as in Table 1 and preparation method as in the previous section were applied.

2.2. Experimental methods

Electrophoretic mobility of colloidal particles and conductivity of dispersions were measured with a DELSA 440SX (Coulter). Undiluted samples were used for measuring the conductivity while only the most turbid samples were diluted in order to perform mobility measurements. The mobility was determined from a Lorentzian fit to the measured peaks at four scattering angles; the corresponding four values of the mobility were averaged.

Static light scattering (SLS) was done using a FICA 50 setup. The aggregated samples were diluted in order to avoid

Table 2
Dilutions with pure ethanol made from the original mixtures in Table 1, used for experiments in which light scattering was involved

Diluted sample	Sb_1	$S3_1$	$S6_1$	$S6_2$	$S7_1$	
Proportion (ml mixture : ml ethanol)	0.4:10	0.2:10	0.2:10	1.5:10	0.25:10	
Used mixture	Sb	S3	S6	$S6_1$	S7	
Diluted sample	$S7_2$	$S8_1$	$S8_2$	$S10_1$	$S13_1$	$S15_1$
Proportion (ml mixture : ml ethanol)	1:10	0.5:12	1:4	1:20	1:20	1:20
Used mixture	$S7_1$	S8	$S8_1$	S10	S13	S15

multiple scattering. The preparation of the mixtures avoided dust as much as possible, so that the samples were not filtered prior to the measurements in order to keep the microstructural properties unaltered. The wavelength of the incident linearly polarized light was $\lambda_0 = 546$ nm. Dynamic light scattering (DLS) was done with a home made setup using a Malvern 7032 CE correlator (128 channels) on the same samples. Different degrees of dilutions of turbid samples were measured (see Table 2). The wavelength of the incident linearly polarized light was 514.5 nm.

Sedimentation in gravitational field was studied on samples stored in a temperature controlled dark chamber (at 20 °C). Cylindrical sedimentation tubes containing 5 ml of samples were used. Pictures were taken regularly.

Particle sizes were determined using an atomic force microscope (AFM) (Nanoscope IIIa, Digital Instruments), in tapping mode, according to [12]. In order to image the cluster formation as well as single particles in the ethanol based samples, we used the cryogenic transmission electron microscopy (cryo-TEM). A "Quantifoil" carbon film was subjected to glow discharge to be made hydrophilic. The sample was prepared in a so called vitrification robot: the film was successively immersed in the dispersion, blotted with filter paper (once for one second in our experiment), and vitrified by shooting it into liquid ethane. In order to prohibit solvent evaporation, the atmosphere was saturated with ethanol vapor. We imaged the particles in the thin ice film formed in the holes (2 μm in diameter) of the carbon film. A transmission electron microscope (Tecnai 12, FEI) equipped with a cryo-holder (626 cryotransfer system, Gatan) were used at low dose conditions to avoid melting the frozen dispersion film. For example, at a magnification of 21,000 the dose was of about 5 electrons per $Å^2$. The exposure time was 500 ms on a high sensitivity CCD camera (TIETZ). The acceleration voltage was 120 kV and the temperature of the sample −180 °C.

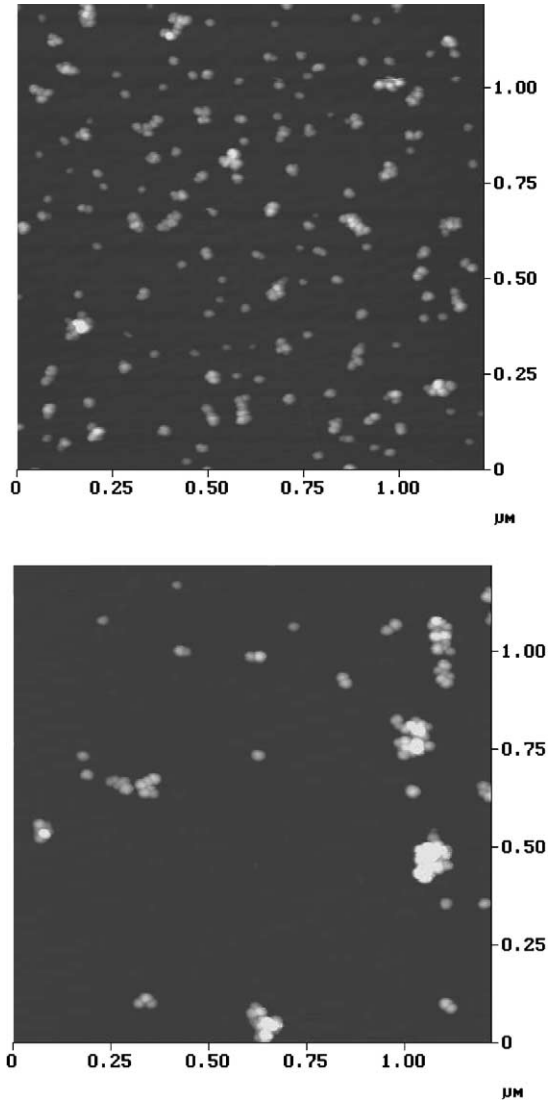

Fig. 1. Height AFM images of negative Ludox particles (above) and positive Ludox particles (below), taken after the particles were transfered to ethanol.

3. Results and discussion

AFM was used to determine the average diameter of particles. For this purpose we used the height image (Fig. 1). Since the lateral diameter is strongly affected by tip convolution, height information was used to determine the particle size [12]. The average diameter of particles was 12.1 nm for negative particles (which confirms the nominal diameter reported by DuPont) and 15.2 nm for positive particles. The latter is larger, due to the alumina layer which covers the silica cores. The determined polydispersity was in both cases of approximately 18%.

Direct observation of series I during the preparation and sedimentation (Fig. 2) showed that the samples Se up to Sa (such subseries will be denoted by Se–Sa), S2 and S3 are unstable: even after a small quantity of positive dispersion

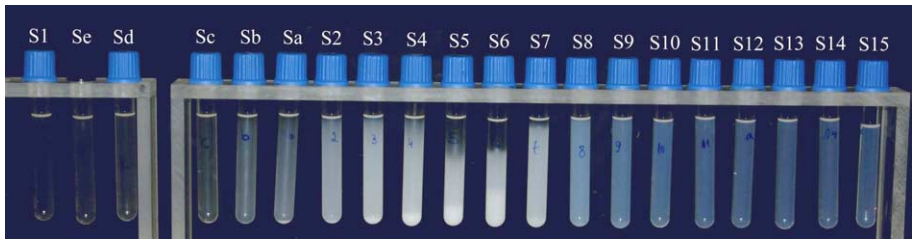

Fig. 2. First series (series I) of mixtures of negative and positive silica particles, 4 days after preparation. The sample composition is indicated in the same order in Table 1.

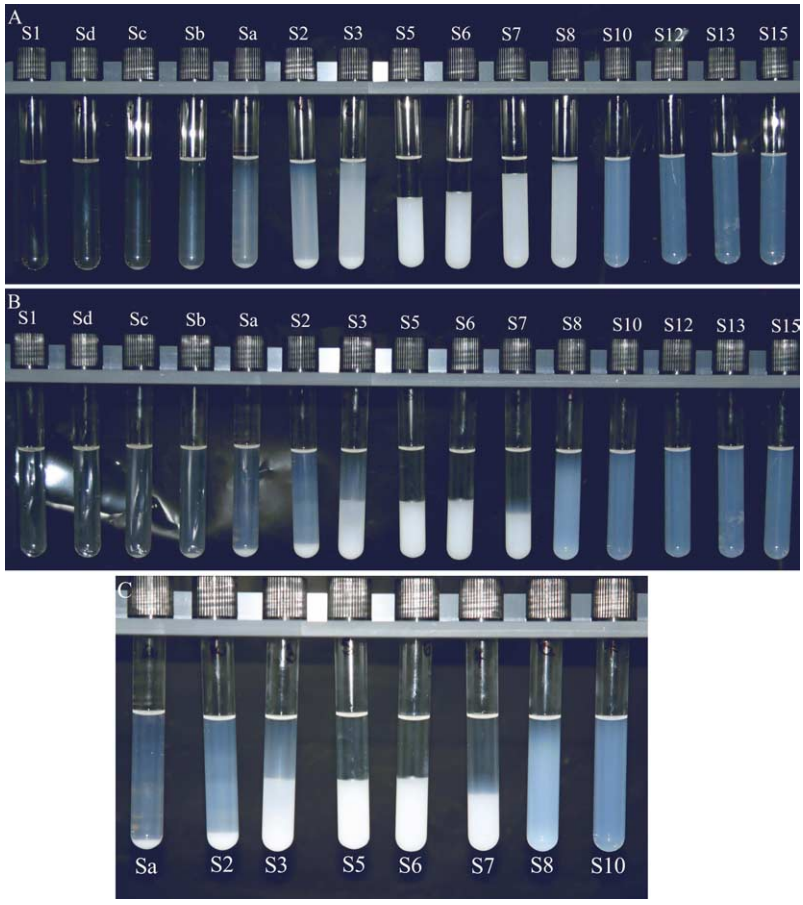

Fig. 3. Pictures of the second series of mixtures (series II) of negative and positive silica particles, taken one week after preparation (A), 5 weeks after preparation (B), and a zoomed in—picture obtained from B for samples Sa–S10 (C). The sample composition is indicated in the same order in Table 1.

was mixed and stirred with the negative dispersion, density fluctuations and aggregate formation were observed (by eye) and the aggregates sedimented fast. Surprisingly, even after larger quantities of negative dispersion were mixed and stirred with the positive dispersion (S8–S14), homogeneous suspensions formed after stirring, in spite of the fact that aggregation was observed as soon as negative particles were injected, as in all mixtures. Only samples S8 and S9 have an increased turbidity in comparison with the positive dispersion S15, indicating the presence of somewhat larger clusters. Samples S2–S7 are very turbid and contain thus very large clusters. Sedimentation was observed in samples Sd–Sa and S2–S7, but no sediment formed in S8–S14.

For *series II* only minor differences were observed in comparison to series I, and this could be due to the small differences in the process of transferring the particles to ethanol. Several pictures of the mixtures were taken after one week, five weeks, and three months, respectively. In comparison with series I, in Fig. 3A (taken after one week) one can observe a similar behavior in the case of samples Sd–Sa, S2–S7, and S10–S13, respectively. In the case of S5 and S6 the supernatant was clear while S8 and even S10 scatter more than in the previous series.

Fig. 3B, taken five weeks later, shows interesting changes in some mixtures: samples S8 and S10 became significantly less turbid indicating a redispersion (repeptization) of ini-

tially clustered particles; the sedimentation velocity of S7 increased in comparison to Fig. 3A; the supernatants of S2 and S3 showed different layers. We can conclude now that the samples S8–S14 are stable suspensions.

The final observations can be summarized as follows. We mention that the picture of series II, taken three months after the preparation, does not show notable changes in comparison with Fig. 3B: (a) Samples S13–S10 are homogeneous and no sediment is observed; (b) Sample S8 shows no sediment; (c) Sample S7 shows sediment and a concentration profile of the supernatant. The sediment presents yield stress, which was also observed for the following discussed samples; (d) Samples S5 and S6 are sedimented but their supernatant does not scatter light; (e) Samples S3, S2 and Sa show sediments and supernatants with several layers; (f) Samples Sb–Sd show sediments and homogeneous supernatants. The supernatant of samples Sb and Sc was subjected to DLS measurements which showed that it contains only negatively charged particles (see Section 3.1).

After three months, all samples were shaken up and stored to observe once more the process. Except for sample S7, which showed a lower sediment volume and somewhat lower turbidity, the observations (a)–(f) were reproduced for all the other samples.

Finally we added positive and negative dispersions (samples S15 and S1, respectively) to the mixture S6 in order to see if mixtures with other composition can be reobtained in this way. The mixture S12 was very well reproduced: the existing aggregates in S6 redispersed after the positive dispersion was added and the obtained sample showed (after a couple of days) a similar turbidity as the directly prepared S12. When we added negative dispersion, the mixture Sa was not so well reproduced. In comparison with the directly prepared Sa, a larger volume of sediment was observed.

Electrical conductivity of dispersions is determined mainly by the concentration and the mobility of the free ions in the solvent. The mobility of colloidal particles is negligible due to their much larger radius. However, the particles may influence the conductivity because they may produce significant electric fields in the suspension if their volume fraction is high enough. A recent analytical study [13] of conductivity and mobility of colloids led to closed-form equations for interacting particle suspensions but valid for low zeta potential (smaller than 25 mV). As we will see, the zeta potential is not low in our systems, so that here only a simple model will be used for conductivity. As it is shown in Fig. 4, the conductivity decreases nonlinearly with the volume fraction of negative particle dispersion Φ_d, while a linear variation was expected for the nonaggregated mixtures, since ion recombination is unlikely to occur. In the aggregated mixtures a release of ions (from the vicinity of a single particle) because of cluster formation may occur and could explain qualitatively the results. In the case of series II a slight initial increase could be observed. However, in this case, the small increase can be a result of evaporation of ethanol due to the small amounts of mixtures prepared

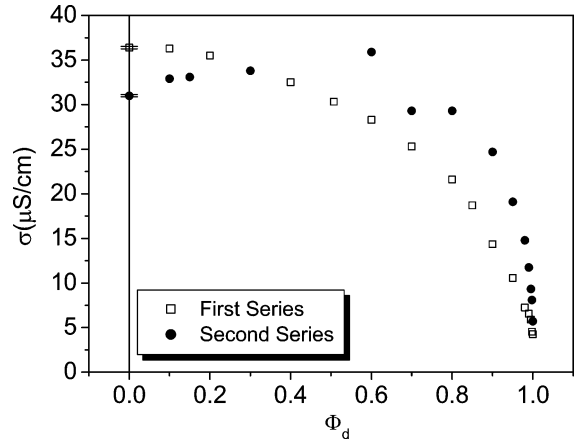

Fig. 4. Conductivity of the mixtures of negative and positive dispersions versus the relative volume fraction of negative particle dispersion.

(the measurements were performed five weeks after preparation, period in which the vials were opened a few times for light scattering measurements). This fact affected also the reproducibility of measurements on series II (the values were somewhat larger after a new measurement) except for the stock sample, so that, in the case of the second series, the error bar is valid for the stocks samples (S15 and S1) only. Series I was measured immediately after the preparation.

Conductivity measurements may be used to estimate ion concentration in the positive and negative dispersions (S15 and S1, respectively), if the ion mobility is known,

$$n_0 = \frac{\sigma}{e(\mu_+ + \mu_-)}, \tag{1}$$

where σ is the conductivity of dispersion, e is the elementary charge and $\mu_{+,-}$ the mobilities of positive and negative ions. As discussed in the beginning of this paragraph, Eq. (1) is valid for low volume fractions of colloids. In addition it may be used for low ionic strength only (when ion–ion interaction is negligible). In comparison with water based samples, the conductivity of ethanol based dispersions is two orders of magnitude smaller.

At this stage determination of the screening length in the colloidal dispersions is useful. The Debye screening length is given by

$$\lambda_D = \frac{1}{\kappa} = \left(\frac{\varepsilon_0 \varepsilon_r kT}{2e^2 n_0}\right)^{1/2}, \tag{2}$$

where ε_0 is the permittivity of vacuum, ε_r the relative permittivity of the solvent (ethanol), k the Boltzmann constant, and T the absolute temperature. The mobility of ions in ethanol (at infinite dilution) in the positive particle dispersion were taken from [14]. The results are presented in Table 3. For negative particles, an estimation was done since the mobilities were not known exactly. In both cases $\kappa R < 1$, where R is the radius of a particle. The particle radius and ion concentration are both relatively small, in agreement with $\kappa R < 1$, hence the Debye–Hückel approximation is ex-

Table 3
AFM radius R_{AFM}, Debye length λ_D, surface potential Φ_0, maximum electrostatic interaction energy $U_{el}(0)$, and charge Q for the negative and positive particles dispersed in ethanol

Sample	R_{AFM} (nm)	λ_D (nm)	Φ_0 (mV)	$U_{el}(0)$ (kT)	Q
Positive particles	7.6	9.0	76.6	14.5	$18\|e\|$
Negative particles	6.1	17.5	−76.6	11.6	$10e$

pected to be valid, even if the electrostatic potential is no longer small [15].

Electrophoretic mobility measurements, done several days after the preparation of mixtures, showed that the sign of particle surface charge does not change after the transfer from water to ethanol. According to the discussion and results in the previous paragraph, the condition $\kappa R < 1$ is achieved, so that the Hückel equation for mobility of colloids

$$\mu = \frac{2\varepsilon_0\varepsilon_r\zeta}{3\eta} \tag{3}$$

should provide reasonable results for both positive and negative colloids. For the aggregated mixtures it cannot be used. In Eq. (3), ζ is the zeta electrostatic potential, which in the case of organic media is usually approximated with the surface electrostatic potential Φ_0 [2]. By determining the surface potential from Eq. (3) (see Table 3), we can calculate the electrostatic attraction energy between a positive and negative particle. The diameter is similar (assumed 13.5 nm in the following calculation) and the absolute values of the surface potentials are the same because the mobilities have practically the same absolute values. For the case $\kappa R < 1$, the DLVO electrical double-layer interaction energy [15] changes only its sign,

$$U_{el}(x) = -\frac{4\pi\varepsilon_0\varepsilon_r R^2\Phi_0^2}{x}\exp\left(-\frac{x-2R}{\lambda_D}\right), \tag{4}$$

where x is the center-to-center distance between two particles. For particles in contact, the result is independent of the Debye length and we found that the interaction energy is $U_{el}(0) = -13kT$. The attraction can be somewhat weaker because of neutralization of the charges which get in contact. In Table 3, the maximum double-layer repulsive energy is presented separately for positive and negative particles. The distance λ_i between the particle surfaces at which the electrostatic attraction energy is equal to the thermal energy (which we call the interaction length) can be estimated easily if we consider the case of a small amount of negative dispersion introduced in the positive dispersion (e.g., S14). Then the Debye length is practically the same as that for the positive dispersion (Table 3) and one obtains $\lambda_i = 16$ nm. These results clearly show that the electrostatic attraction will coagulate the positive and negative particles if the distance between their surfaces is comparable with the Debye length. It remains to be explained why samples S8–S14 are so stable and why the aggregated particles can redisperse.

The mobilities for the two series of mixtures presented in Fig. 5 give valuable information to account for stability as

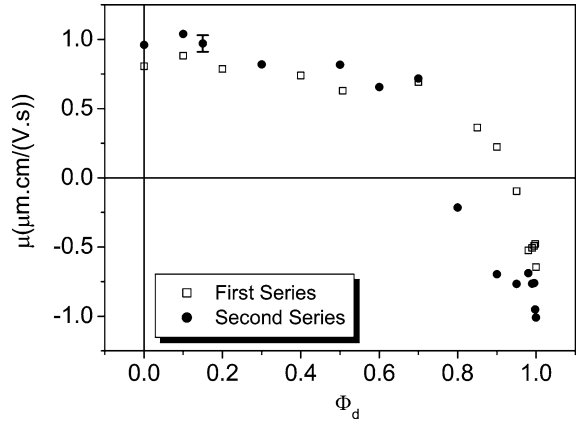

Fig. 5. Electrophoretic mobility of the mixtures of negative and positive dispersions versus the relative volume fraction of negative particle dispersion.

well as for structures in the aggregated samples, respectively. The trend for both series is similar. A higher absolute value of the mobility of negative particles in the second series is observed, which can explain the shift of the zero mobility point to the left (for this series).

Samples S8–S15 exhibit positive mobilities of colloids, with close values, but a small decrease can be observed. Taking also into account that they are stable and no sediment was observed, we may conclude that either the negative particles are well screened by the positive particles in a small cluster or the negative particles somehow become positive. The second hypothesis may be true only for a limited amount of negative particles dispersed in the positive system otherwise we cannot explain the instability of samples Se–Sa. Surprisingly, samples S7 and S6, which are strongly aggregated, show similar positive values of the electrophoretic mobilities. We may assume in this case that the charges in a cluster cancel out and most of the particles in the outer layer are positively charged. Hence, the mobility, determined only by the surface potential of aggregates, is close to that of single positive particles.

At higher values of Φ_d, the mobility sharply decreases becoming negative. The unstable samples S2 and Sd–Sa exhibit negative values of mobilities close to the mobility of the single negative particles in the sample S1. The negative mobility for aggregated samples can be explained in the same way as above, but now most of the particles in the outer shell of the clusters are negatively charged.

In the vicinity of the volume fraction of negative dispersion of $\Phi_d = 0.78$, the mobility is close to zero. That means that the net charge of particle clusters is very small. The outer shell is composed of both positively and negatively

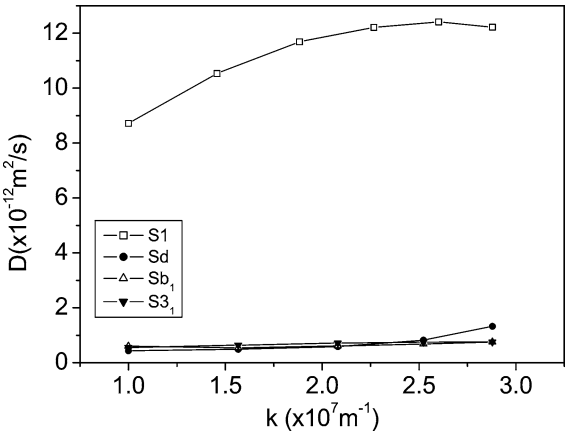

Fig. 6. Diffusion coefficients versus scattering vector obtained from DLS measurements for negatively charged particles and mixtures containing a small quantity of positive dispersion.

charged particles. This may explain why the largest aggregates formed in samples with Φ_d close to the value of 0.78.

Light scattering was performed on samples of series II, a few days after the preparation. When the turbidity was too high, we measured diluted samples, marked with index 1 or 2 according to Table 2, in order to avoid multiple scattering. This fact may have an influence on the dimension of aggregates but we will make comparisons between diluted samples.

SLS performed on samples Sb_1, $S3_1$, $S6_1$–$S8_1$ shows no minima in their angular intensity profile, which points to a large polydispersity of aggregates in size and shape. The DLS measurements are discussed in detail below.

In Fig. 6 the diffusion coefficients for samples S1, Sd, Sb_1 and $S3_1$ are presented. The radius of particles in sample S1 varied (with the increasing scattering angle) between 22 and 16 nm, which exceeded the size measured with AFM. The same result was obtained after the sample was highly diluted and after a high dilution of the original aqueous dispersion was measured. The size determined from DLS (which is always larger than the AFM or TEM one) was however beyond our expectancy. This is most probably due to some aggregates present in these samples, also observed in the cryo-TEM image (Fig. 7D), in which we found indeed aggregates with radii of about 16 nm or larger. The polydispersity of single particles, of aggregates, and also the possible presence of some residual impurities explain the dependence of the diffusion coefficient on the scattering angle.

Much lower diffusion coefficients than in the case of sample S1 were obtained for Sd, Sb_1, and $S3_1$ as a result of significant aggregation. These results are rather qualitative, taking into account the poor stability of these samples. It is thus clear why the dynamical contrast of measurements and the fit with the intensity autocorrelation function (IACF) [16] for monodisperse spheres were not so good. Qualitatively, the above mentioned diffusion coefficients show that even small volumes of positive dispersion mixed with S1, lead to large aggregate formation. Thus, the positive parti-

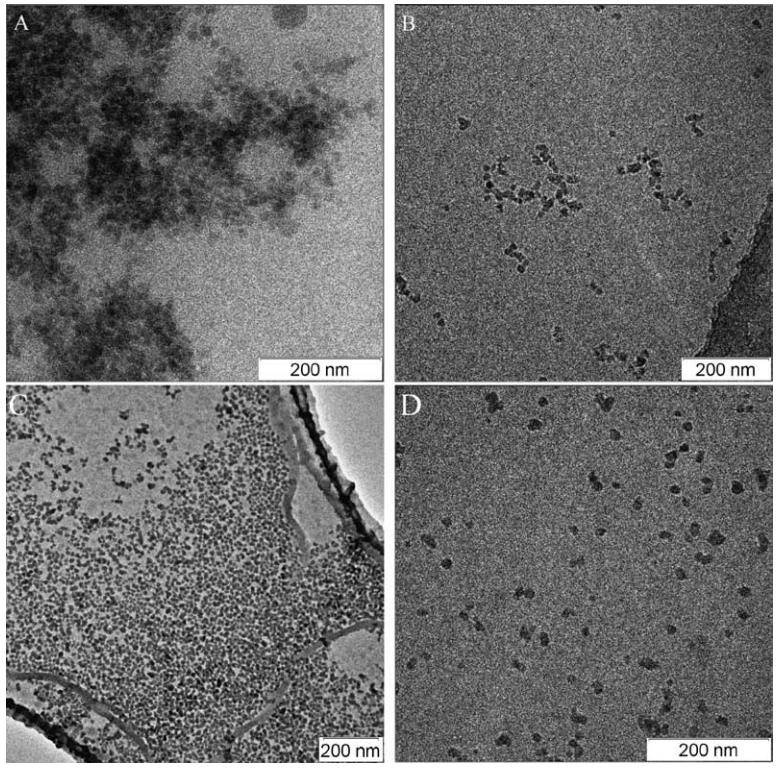

Fig. 7. (A, B) Cryo-TEM pictures of sample S2, which is a mixture of negative and positive particles as indicated in Table 1. (C) TEM picture of S2 (the specimen was dried in air). (D) Cryo-TEM picture of sample S1, which contains only negatively charged particles.

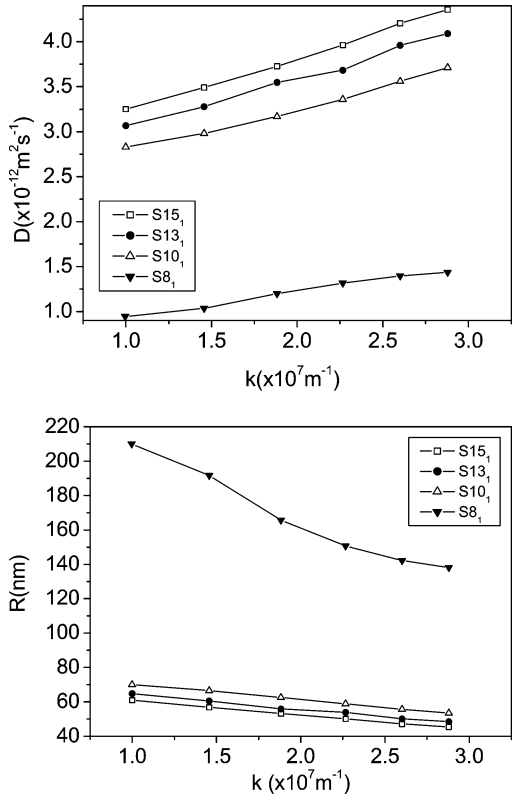

Fig. 8. Diffusion coefficients D and particle radius R versus scattering vector obtained from DLS measurements for positively charged particles and mixtures containing positive dispersion down to 50%.

cles are not screened by the negative ones and the cluster growth does not stop at an early stage.

In Fig. 8 the results for samples $S15_1$, $S13_1$, $S10_1$, and $S8_1$ are presented. The radius of positive Ludox particles (between 65 and 45 nm, depending on the scattering angle) was determined using S15, several dilutions of S15, as well as a very diluted aqueous sample (obtained directly from the original Ludox dispersion) without noticeable differences. The DLS radius of positive particles is larger than that of negative particles. The same explanations for the larger size of positive particles compared to the AFM size and for the dependence on scattering angle, mentioned above for negative particles, are assumed.

Samples $S13_1$ and $S10_1$ show negligible differences in diameter of particles in comparison with $S15_1$ and the same polydispersity. Only $S8_1$ contains significant heteroaggregates. A higher dilution of S8 led to approximately the same results as $S8_1$. All these samples led to a good fit with IACF for monodisperse spheres, and the measurements showed a very good dynamical contrast which make these results quantitatively more accurate.

From mobility measurements we concluded that the stability of these samples is either due to a proper screening of negative particles (which stops the growth of clusters) or due to their recharging. If the negative particles are screened and are surrounded by positive particles, then we should see a larger radius in the DLS measurements of samples S13

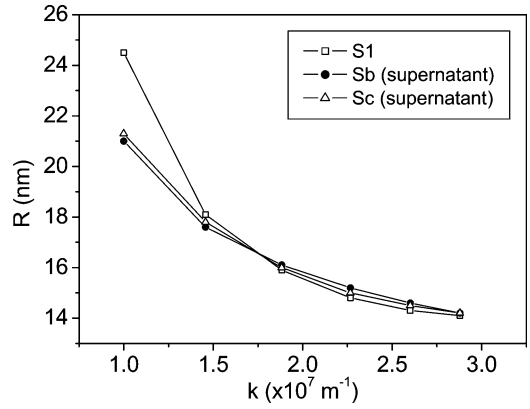

Fig. 9. Radius of the negative particles determined from DLS measurements using the supernatant of samples Sb and Sc as well as the sample S1.

and S10 for example, in comparison with that measured for S15. Referring to the sample S10, the ratio of positive to negative particles, without taking into account primary aggregates, is approximately 2.3 and it is not easy to understand how such a ratio can result in a sufficient screening. The hypothesis of recharging of negative particles should thus receive more attention (see Section 3.1).

It is also interesting to mention that in the case of samples Sc and Sb, the supernatant contains only negative particles, according to the DLS determination of radius (Fig. 9), done three months after the preparation. The larger value of radius at the smallest angle, for sample S1, is due to the homoaggregation process: this sample was shaken up before the measurement while the upper part of the supernatant of samples Sc and Sb was extracted with a syringe. The homoaggregation process is thus measurable at small angles but is very weak. From Fig. 9 we can infer that all positive particles are clustered and sedimented, so that, indeed, in these samples the growth of aggregates does not stop at a small cluster size.

TEM and cryo-TEM. Since the diameter of positive and negative particles is similar, we expect fractal like clusters in samples Sd–Sa and S2–S7. Optical microscopy investigations suggested that this is indeed the case, but the confirmation we give is obtained by using the cryo-TEM technique. The images of sample S2 (Fig. 7A) show large fractal cluster formation, although, some areas show the presence of small fractals or chains (Fig. 7B). Fig. 7C presents for comparison a conventional TEM picture of S2, i.e., the image of a specimen prepared after the colloid thin film was dried in air. The contrast is better in this case since the constraint of low dose is not required anymore. The cryo-TEM picture of the sample S1 (Fig. 7D) shows single particles, except for some homoclusters also observed in DLS experiments.

3.1. Repeptization and stability of mixtures

We deal here in more detail with the unexpected stability of samples S8–S14. According to the discussions in the previous subsection, the stability is very likely due to a "charge-inversion" of negative particles to a posi-

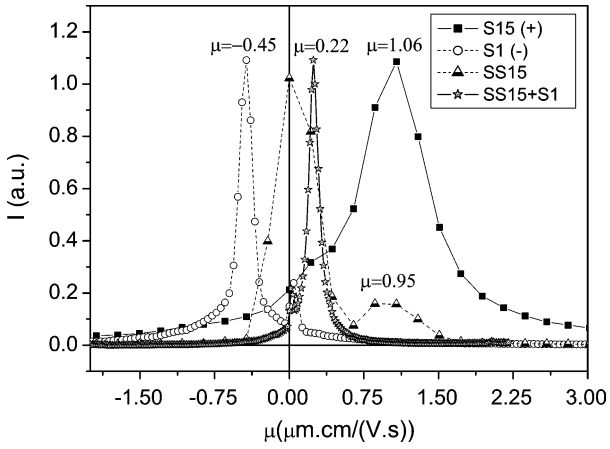

Fig. 10. Electrophoresis measurements on positive particles (S15), negative particles (S1), supernatant of the sedimented positive particle dispersion (SS15), and negative particles dispersed in that supernatant (SS15 + S1).

tive value. To verify this hypothesis, the following experiments were done three months after the preparation of samples. No noticeable changes were observed after this time in the mobility of positive particles (the remeasured value was $+1.06$ μm cm/(V s)), while an increase to -0.45 μm cm/(V s) was noticed for negative particles. The positive dispersion S15 was sedimented by ultracentrifugation (25000 rpm, 4 days). The supernatant was removed and subjected to an electrophoresis measurement. It showed a peak corresponding to zero mobility, but also a small one corresponding to the mobility of positive particles. The negative particle dispersion was added ($\Phi_d = 50\%$) to the supernatant. Initially an increase in the turbidity was observed (due to aggregates) but after a few hours the aggregated particles redispersed. The electrophoretic measurements showed now a peak corresponding to a mobility of $+0.22$ μm cm/(V s) and no peaks in the negative mobility region. These results are presented in Fig. 10. Recharging of initially negative particles is not due to the slightly acid pH of the supernatant used in the above mentioned experiment. We added HCl to the negative dispersion in different concentrations, measured in terms of conductivity. At the values of conductivity similar to or larger (up to one order of magnitude) than the conductivity of the supernatant, no change in the mobility was observed. Only when much more HCl was added (conductivity of order of mS/cm) the mobility was close to zero. This behavior of silica mobility versus pH, in ethanol, is actually known and we reobtained the results presented in [2]. It is known that the solubility of silica in ethanol is very small [17], but alumina may dissolve significantly, resulting in positively charged aluminate species, which adsorb onto the negative silica particles and change their charge. It was observed that the process of repeptization depends on concentration and composition of mixtures being much faster at small values of Φ_d. Probably, after positive charges are adsorbed, more alumina dissolve, until a final equilibrium is reached. For samples S2–S7, the recharging phenomenon should occur too, but because the volume of positive dispersion is smaller, there were not enough ions for the negative particles to be recharged. Thus fractal aggregation persisted in time together with instability.

The charge of particles before the mixture were prepared can be determined in the frame of the Debye–Hückel model, discussed in the previous section:

$$Q = 4\pi\varepsilon_0\varepsilon_r\Phi_0 R\left(1+\frac{R}{\lambda_D}\right). \tag{5}$$

Using the determined Debye lengths and surface potentials, we obtained for the particle charges the results presented in Table 3. Consequently, there should be more than 10 positive monovalent ions in the solvent of positive dispersion for each negative particle for the redispersion to be possible. As will be discussed below, the van der Waals attraction energy in these systems is comparable with kT.

The total DLVO potential energy U_{tot} [15] for two single initially negative particles is obtained by adding the van der Waals energy U_{W} to Eq. (4) taken now with the sign changed,

$$U_{\text{W}}(x) = -\frac{A}{6}\left[\frac{2R^2}{x^2-4R^2}+\frac{2R^2}{x^2}+\ln\left(1-\frac{4R^2}{x^2}\right)\right], \tag{6}$$

where A is the Hamaker constant and x is the center-to-center distance between the two particles. The electrostatic energy is calculated using the parameters determined for negative particles (presented in Table 3). The Hamaker constant for silica in ethanol was calculated by using the Lifshitz model [18],

$$A = \frac{3}{4}kT\left(\frac{\varepsilon_1-\varepsilon_2}{\varepsilon_1+\varepsilon_2}\right)^2+\frac{3h\nu_e}{16\sqrt{2}}\frac{(n_1^2-n_2^2)^2}{(n_1^2+n_2^2)^{3/2}}, \tag{7}$$

where ε_1 and ε_2 are the static dielectric constants of ethanol and silica, respectively, n_1 and n_2 are the refractive indexes of ethanol and silica (in the visible spectrum), h is the Planck constant, and ν_e is the main electronic absorption frequency in the UV (of the order of 3×10^{15} Hz). A barrier of energy of the order of $10kT$ resulted from this calculation, as expected (not presented).

It is interesting to see if the theory supports the redispersion of heteroaggregated particles. According to the electrophoretic mobility measurements, the initially negatively charged particles recharge to a surface potential equal to $\Phi_0' = 16.9$ mV (obtained by using Eq. (3)). This surface potential corresponds to a charge of $Q = +4|e|$. In this case Eq. (4) is not valid anymore because of the quite large difference between the surface potential of the positive particle ($\Phi_0 = 76.6$ mV) and of the recharged particle ($\Phi_0' = 16.9$ mV). For the case of two particles with the same radius and Debye length, but different surface potentials, the electrostatic potential energy is given by [19]

$$U_{\text{el}}'(x) = 2\pi\varepsilon_0\varepsilon_r R\Phi_0\Phi_0'\exp\left(-\frac{x-2R}{\lambda_D}\right). \tag{8}$$

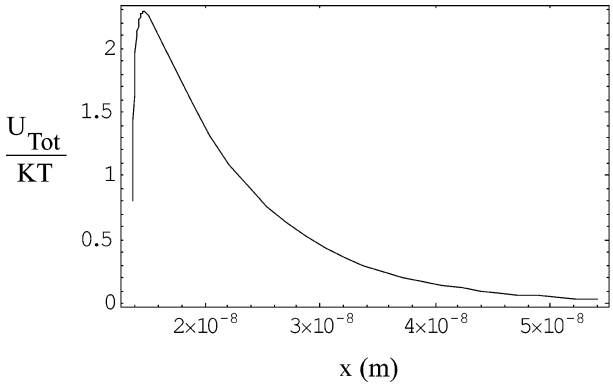

Fig. 11. Total DLVO potential energy per kT of a positive particle and a recharged particle versus center-to-center distance. The minimum distance between the particle surfaces was 0.23 nm.

Equation (8), which is correct for $\kappa R > 1$, is assumed to give good qualitative results for the case $\kappa R < 1$. In a cluster, multiple interactions should be taken into account. Accordingly, the results discussed below can be regarded as an estimation for the case of a heteroaggregate composed by two particles. We may think to a mixture with only a small amount of negative dispersion, such as S14. In this case the Debye length is practically the same as that one for positive particles (see Table 3). By using Eqs. (6), (7) and (8) the total potential energy, presented in Fig. 11, shows only repulsive interaction if there is a minimum distance between the surfaces of the particles (in Fig. 11 the minimum distance was 0.23 nm). This minimum distance may come from the surface roughness of the particles. It cannot be excluded that also the alumina layer plays a role in reducing van der Waals interaction, such thin layers being usually porous.

We observed that the van der Waals energy is comparable to kT in the initial positive and negative dispersions, respectively: after salt ($LiNO_3$) was added in high enough concentration (of order of 0.1 M), no flocculation or aggregation was observed by eye. The turbidity of positive dispersion only slightly increased after a period of 10 days but the system remained stable. When the positive and negative dispersions were mixed, aggregates were not observed either (however, they appeared one week later making the mixture turbid). Thus the particle charge was screened well and if van der Waals had been significantly larger than kT the systems would have flocculated. The DLVO total potential energy for the positive and negative dispersions, respectively, after salt was added, showed indeed a very thin residual electrostatic barrier of the order of kT, while for surface-to-surface distances larger than 0.1 nm, the total interaction potential is larger than $-kT$. This shows that in the systems studied in this paper the particle association/dissociation is practically controlled by the electrostatic interactions.

Salt effect. Electrostatic interactions between particles can be adjusted by adding certain amounts of salt. $LiNO_3$ was added to samples S1 (the negative dispersion) and S15 (the positive dispersion) which were subsequently mixed at volume ratios of 3:1.3 (the composition corresponds to aggregated sample S6, Fig. 12B) and 1.3:3 (the composition corresponds to stable sample S10, Fig. 12A). Fig. 12A shows that salt addition prohibits the repeptization. The aggregates persist in time and sediment, the profile of sedimentation being dependent on the salt concentration. This could be explained by the fact that a higher density of positive ions surround the negative particles preventing the absorption of aluminate positive ions and the repeptization. Fig. 12B shows the opposite effect of salt in sample S6. The increasing salt concentration up to 0.3 M reduces the heteroaggregate formation. Beyond this limit, somewhat large heteroclusters form because the salt dissociates less at high concentrations. However, all sediments observed still present yield stress.

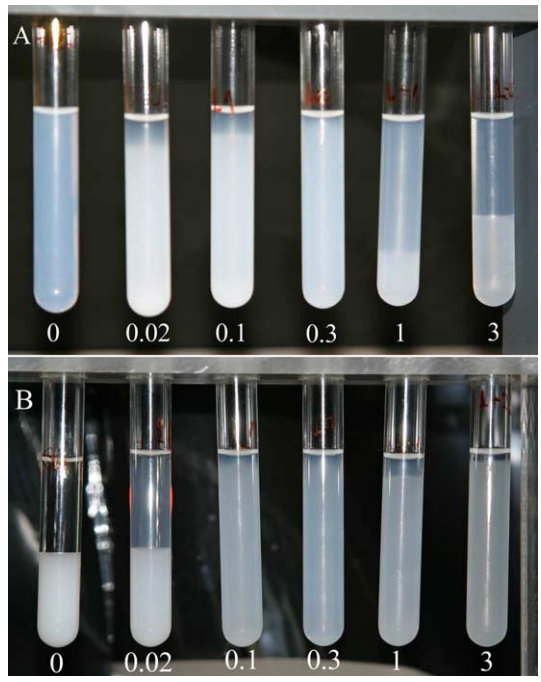

Fig. 12. Effects of salt addition on the stable sample S10 (A) and on the aggregated sample S6 (B). The molar salt concentration is indicated by the numbers in the two pictures.

4. Conclusions

Mixtures of initially oppositely charged silica particles were studied at low ionic strength. Heteroaggregation was observed in the group of mixtures with smaller positive particle content while stability and only relatively small aggregates, which decayed in time were observed in the rest of the mixtures.

The particle repeptization and the stability of the samples containing up to 50% initial negative dispersion can be explained by the recharging of the negative particles as a result of adsorption of aluminate species. This explanation was confirmed after the negative particles were dispersed in the solvent of the positive dispersion and the electrophoretic mobility was measured, and is consistent with the electrophoresis and light scattering measurements done on these group

of mixtures. The time-dependent process of aggregate redispersion scales with the volume ratio of the mixtures.

Mixtures with a higher negatively charged particle content exhibited large aggregates. When only a small amount of positive particle dispersion is present (down to approximately 0.2%), the samples were unstable and all positive particles aggregated and sedimented. When the amount of positive particle dispersion was higher (up to approximately 15%) the sediment, which presented yield stress, was accompanied by various supernatant profiles.

The conductivity of the series of mixtures showed a nonlinear behavior versus the volume fraction of negative dispersion Φ_d while the electrophoretic mobility measurements showed a zero point mobility around $\Phi_d = 78\%$. In this case we assumed that the particles in the outer shell of the clusters are both negative and positive so that the surface potential is close to zero. In the case of unstable samples most of the particles in the outer shell of the clusters are negatively charged (since a negative mobility was measured) but that was not enough however for achieving stability.

The Debye length, particle charge, and DLVO potential energy were determined and discussed for the unmixed particles. The calculated total potential energy for a positive particle and a recharged particle (which have different surface potentials) supports quantitatively the particle redispersion form heteroaggregates. In the investigated systems, the particle association/dissociation is practically controlled by the electrostatic interaction. Salt addition had opposite effects on the stability of initially unstable and stable mixtures, respectively.

Acknowledgments

Dr. B. Erné and N. Zuiverloon are thanked for helpful discussions. This work was financially supported by NWO–CW (Nederlandse Organisatie voor Wetenschappelijk Onderzoek–Chemische Wetenschappen).

References

[1] K. Furusawa, C. Anzai, Colloids Surf. 63 (1992) 103.
[2] G. Wang, P. Nicholson, J. Am. Chem. Soc. 84 (2001) 1250.
[3] A.Y. Kim, J.C. Berg, J. Colloid Interface Sci. 229 (2000) 607.
[4] A.Y. Kim, K.D. Hauch, J.C. Berg, J.E. Martin, R.A. Anderson, J. Colloid Interface Sci. 260 (2003) 149.
[5] A.M. Puertas, A. Fernandez-Barbero, F.J. de las Nieves, J. Chem. Phys. 114 (2001) 591.
[6] A.M. Puertas, A. Fernandez-Barbero, F.J. de las Nieves, Physica A 304 (2002) 340.
[7] W.L. Yu, M. Borkovec, J. Chem. Phys. B 106 (2002) 13106.
[8] A.M. Islam, B.Z. Chowdhry, M.J. Snowden, Adv. Colloid Interface Sci. 62 (1995) 109.
[9] S. Usui, Prog. Membrane Surf. Sci. 3 (1972) 223.
[10] C. Pathmamanoharan, A.P. Philipse, J. Colloid Interface Sci. 165 (1994) 519.
[11] H.J. van den Hul, J.W. Vanderhoff, J. Colloid Interface Sci. 28 (1968) 336.
[12] M. Rasa, B.W.M. Kuipers, A.P. Philipse, J. Colloid Interface Sci. 250 (2002) 303.
[13] H.J. Keh, J.M. Ding, Langmuir 18 (2002) 4572.
[14] G. Kortüm, Treatise on Electrochemistry, Elsevier, Amsterdam, 1965, p. 252.
[15] E.J.W. Verwey, J.Th. Overbeek, Theory of the Stability of Lyophobic Colloids, Dover, New York, 1999.
[16] J.K.G. Dhont, An Introduction to Dynamic of Colloids, Elsevier, Amsterdam, 1996, p. 144.
[17] P.A. Buining, L.M. Liz-Marzan, A.P. Philipse, J. Colloid Interface Sci. 179 (1996) 318.
[18] J. Israelachvili, Intermolecular and Surface Forces, Academic Press, London, 1992, p. 183.
[19] A.M. Puertas, A. Fernandez-Barbero, F.J. de las Nieves, J. Chem. Phys. 115 (2001) 5662.